Rapid hybrid microwave cladding of SiO_2/TiO_2 sol-gel derived composite coatings

Ka-Wai Yeung[a], Ling Chen[b], Chak-Yin Tang[a]*, Man-Tik Choy[a], Akeem Damilola Akinwekomi[c], Wing-Cheung Law[a], Gary Chi-Pong Tsui[a]

[a]Department of Industrial and Systems Engineering, The Hong Kong Polytechnic University, Hong Kong, China

[b]Manufacturing BU, CSIRO, Private Bag 10, Clayton South Vic 3169, Australia

[c]Department of Metallurgical and Materials Engineering, The Federal University of Technology, Akure PMB 704, Ondo State, Nigeria

*Corresponding author

Email address: cy.tang@polyu.edu.hk (Chak-Yin Tang), Phone: +852 2766 6608, Fax: +852 2362 5267

Postal address: Department of Industrial and Systems Engineering, The Hong Kong Polytechnic University, Hung Hom, Kowloon, Hong Kong, China.

Acknowledgements

This work was supported by a grant from the Research Committee of The Hong Kong Polytechnic University under student account code RK20, and the Innovation and Technology Fund under project code ITS/381/14 which was granted by the Innovation and Technology Commission of The Government of the Hong Kong Special Administrative Region.

Highlights

- A hybrid microwave cladding process is developed for the fabrication of composite coating systems with disparate dielectric properties
- The difficulty of processing low microwave absorbing and microwave transparent materials has been overcome
- Fabrication of crack-free silicon dioxide (SiO_2) / titanium dioxide (TiO_2) composite coatings on polycarbonate substrates with enhanced surface mechanical properties has been demonstrated
- This process greatly reduces the processing time from hours to within a minute compared to conventional methods

Abstract

UV protection and coatings for plastics are important for various applications. Cladding of low microwave (MW) absorption composite coatings on high MW transparent plastic substrates is a challenge due to their disparate dielectric properties. Moreover, an uneven heat energy conversion within the composite creates an additional hurdle to produce a coating with good surface integrity. In this study, a protocol was developed to overcome these difficulties based on a hybrid approach. The adverse effect of temperature mismatch between the coating and substrate was reduced through a two-way susceptor-aided heating mechanism. Low MW absorbing sol-gel derived composite coatings consisting of silicon dioxide (SiO_2) and titanium dioxide (TiO_2) were successfully cladded on the surface of MW and visual light transparent polycarbonate to produce a clear protective coating with UV-resistance. Nanoindentation tests were conducted to assess the effectiveness of the proposed protocol. Significant enhancement in the surface elastic modulus and hardness were achieved.

Keywords: microwave; susceptor heating; composite coating; transparent substrate; scratch resistance; UV protection

Introduction

Engineering plastics, such as polycarbonate (PC), have been widely used to produce optical lenses due to their low cost, high clarity, impact resistance and chemical inertness. However, they are susceptible to abrasion damage and photodegradation under UV light, which alters their optical transparency and mechanical properties [1]. Therefore, cladding protective coatings on the surface is crucial to extend the lifespan of a plastic product. Inorganic metal oxide particles, such as silicon dioxide (SiO_2), are commonly used in coating materials because they possess high visible transmittance and can improve the scratch resistance of the surface [2-6]. In addition, titanium dioxide (TiO_2), with an absorption band in the ultraviolet region, has been widely used as a functional additive in, or as a coating material on, polymers to enhance photo-stability [7] and reduce yellowing of polymer substrates [8,9]. UV protection can also provide a long-term adhesive strength of the coating as stress may occur at the coating-substrate interface due to the photodegradation of the polymer substrates [10]. Numerous techniques, for instance, physical and chemical vapor deposition methods, have been developed to apply such coatings [11,12]. However, most of the methods are expensive and require high energy input. Alternatively, SiO_2/TiO_2 composite film can be synthesized on a substrate by bottom-up approaches such as sol-gel method to reduce the production cost [13]. The consolidation of SiO_2/TiO_2 precursors can lead to the formation of inorganic composite film with a three-dimensional atomic structure through a thermal-induced simultaneous hydrolysis and condensation [1].

Microwave (MW) technology has been widely applied in the synthesis of nanomaterials. It has been used in synthetic chemistry due to its high efficiency and accelerated reaction rates [14,15]. During sol-gel synthesis, MW processing may promotes further condensation and offers a higher yield of the product. However, direct MW processing of low MW absorption composite coatings on MW transparent plastic substrate remains challenging due to different dielectric properties and poor microwave absorbability. Several attempts have been made to synthesize sol-gel based SiO_2/TiO_2 coating on MW transparent polymer substrates by direct MW irradiation [16-18]. As the SiO_2 and TiO_2 coating materials coupled weakly with MW irradiation due to their low dielectric loss properties, heat generation was limited. This led to incomplete hydrolysis and condensation of the sol-gel precursors at a relatively low temperature [19]. Therefore, no improvement of surface properties could be made. Another major difficulty was the temperature inhomogeneity during the direct MW heating process. Due to different MW absorption rates of the coating and MW transparent substrate, thermal stress may be generated at the interface, subsequently leading to to coating failures, such as cracking and coating delamination [20].

In this study, a hybrid MW cladding protocol has been developed to overcome these challenges. A kiln made of silicon carbide (SiC) susceptor was introduced into the heating system to investigate a two-way susceptor-aided heating mechanism. During the heating process, the sample was heated volumetrically by means of direct coupling with the MW irradiation, and from the surface by means of the conventional mode of heat transfer from the susceptor. Using the proposed method, sol-gel-derived SiO_2/TiO_2 composite coatings were successfully fabricated in a short period of time. This hybrid heating approach could provide a faster heating rate and better thermal homogeneity between the coating and substrate. The coatings exhibited improved mechanical properties and good UV absorbability with a crack-free surface.

Experimental section

Materials

PC substrates (Lexan XL10) with dimensions of 10 mm (W) × 20 mm (L) × 3 mm (H) were used as the starting substrate material. Potassium dichromate ($K_2Cr_2O_7$, ≥98%, Aladdin), sulfuric acid (H_2SO_4, 95%, AnalaR NORMAPUR) and 3-aminopropyl triethoxysilane ($Si(OC_2H_5)_3(CH_2)_3NH_3$ or 3-APS, ≥98%, Sigma-Aldrich) were used for surface functionalization of the PC. Tetraethyl orthosilicate ($Si(OC_2H_5)_4$, TEOS, ≥98%) and titanium tetraisopropoxide ($Ti(OCH(CH_3)_2)_4$, TTIP, ≥99.5%), purchased from International Laboratory, were used as the precursor for SiO_2 and TiO_2 sol-gel. Ethanol (C_2H_5OH, EtOH, ≥99.8%, Sigma-Aldrich) and 2-propanol ($(CH_3)_2CHOH$, 2-IPA, ≥99.5%, anhydrous, International Laboratory) were used as organic solvents during the sol-gel preparation. 0.1 M hydrochloric acid (HCl, Sigma-Aldrich) and glacial acetic acid (CH_3COOH, ≥99.8%, Sigma-Aldrich) were used as reagents to produce a stable sol for the coating process.

Two-step surface functionalization of PC specimen

Polycarbonate (PC) features low chemical affinity and surface wettability with most coating materials [1]. To improve the adhesion between the composite coating and the PC substrate, a two-step surface functionalization method was developed. All PC substrates were firstly cleaned by compressed air to remove debris on the surface, and then cleaned by detergent and rinsed with distilled water. The substrates were ultrasonically cleaned using 2-IPA for 10 mins, followed by drying under room temperature. After drying, the PC substrates were immersed in a sulfochromic acid solution for 30 mins. The sulfochromic acid solution was prepared by mixing 37.5 ml H_2SO_4 and 4 g $K_2Cr_2O_7$ with 12.5 ml DI water. The acid treated substrates then underwent a second treatment with a silanization solution, which was prepared by mixing 1 g 3-APS with 100 ml of 2-IPA, for 5 mins. The silanized substrates were dried at room temperature prior to use.

Sol-gel preparation and film deposition

The SiO_2 and TiO_2 sol-gels were prepared separately, using TEOS and TTIP as precursors, EtOH and 2-IPA as solvents, respectively. To prepare the SiO_2 sol, TEOS was mixed with EtOH in a molar ratio of 1:10. Subsequently, 0.1 M HCl was added to the mixture until the pH value reached 2. TTIP was mixed with 2-IPA and CH_3COOH in a ratio of 1:35:7 to prepare the TiO_2 sol. The solution was adjusted to pH 4 by adding 0.1 M HCl. Water was added to the solution dropwise to ensure the molar ratio of TEOS:H_2O and TTIP:H_2O was 1:4. The hydrolysis and condensation reactions started once the water was added. Both sols were then aged for 4 hours before depositing onto the substrate.

To study the effect of TiO_2 content on the anti-scratching and UV-blocking capabilities, samples with different coating compositions were prepared, as shown in Table 1. The pretreated PC substrates were dip-coated with the SiO_2/TiO_2 composite sol using the PTL-MM01 dip coater (MTI Corporation) at a withdrawal speed of 3 mm/s. The coated samples were left to dry at room temperature to remove excessive solvent. The process was repeated three times so that three layers of coating were deposited on the PC surface.

Table 1 Formulation of SiO_2/TiO_2 composites

Samples	**Coating compositions**	
	SiO_2 sol (vol. %)	**TiO_2 Sol (vol. %)**
S0 (untreated PC)	---	---
S0-1 (1 step surface treatment)	---	---
S0-2 (2 steps surface treatment)	---	---
S1-0T	100	0
S2-5T	95	5
S3-10T	90	10
S4-30T	70	30
S5-50T	50	50
S6-100T	0	100

Hybrid microwave cladding process

A 2.45 GHz MW furnace (HAMiLab-HV3, SYNOTHERM Corporation) was used for the cladding process. A cylindrical alumina (Al_2O_3) kiln with an inner layer of silicon carbide (SiC) was used as the

MW susceptor. Before the cladding process, the MW furnace was preheated with the kiln for 2 mins using a MW power of 500 W. The temperature was monitored by an infrared sensor. The samples were then put into the kiln and heated under a MW power of 100 W for 30 s at 120 °C.

Characterization

The surface morphology of the coatings was studied using an optical microscope (Leica DM 4000M) and a scanning electron microscope (SEM, JEOL JSM-6490). The coating-substrate interfaces were investigated by the SEM cross-sectional image. The samples were cut in half and the cut surfaces were ground using 400 and 600 grit sand paper. All SEM samples were sputter coated with a thin layer of gold to enhance their conductivity.

The characteristics of the coatings were investigated with respect to their adhesion strength and scratch resistance. A crosscut tape test, in compliance with ASTM D3359-17, was performed to study the adhesion strength between the PC substrate and the coatings. A crosscut tester (QFHD60D, GYX International Instrument Co., Ltd) with a 1 mm cutting space was used to create a 5 × 5 grid for further inspection. The scratch resistance was determined by a pencil hardness tester (Scratch Hardness Tester Model QHQ-A, GYX International Instrument Co., Ltd.) which also conformed to the ASTM standard D3363-05 method.

UV absorption property of the composite coatings was investigated by using an ultraviolet-visible (UV-Vis) spectrophotometer (HR2000, Ocean Optic, USA) in a wavelength range of 300 to 700 nm. The UV absorbability for the aged sol of the corresponding composition was measured.

Nanomechanical performance of the coatings was studied through nanoindentation test by using a Hysitron Inc. TriboScope® nanomechanical test instrument. A three-sided pyramidal diamond cube corner indenter with a 150 nm tip radius was used in the test with a maximum loading force of 400 μN. The instrument was calibrated using fused silica samples prior to the testing. In all tests, a total of 5 indents were made, and the mean hardness (*H*) and elastic modulus (*E*) were evaluated accordingly. Nano-scratch testing was performed using a conical indenter with a tip radius of 1 μm. A progressive normal force from 0 μN to 1000 μN in 5 s was applied to the coating surface with a dwell time of 15 s. Scratches with a length of 6 μm were created. The friction coefficient of the samples was evaluated by taking the ratio of tangential force to the normal load (LF/NF). Three measurements were performed, and the average friction coefficient was calculated accordingly.

Results and discussion

Mechanism of hybrid microwave cladding of SiO_2/TiO_2 composite

During the cladding process, as depicted in Fig. 1a, MW energy was partly absorbed by the SiC when passing through the kiln. As SiC was a high loss material which absorbed MW energy efficiently, a large amount of heat was generated within a few minutes so that a rapid increase of temperature could be achieved [21]. The transmitted MW energy was absorbed by the SiO_2/TiO_2 coating simultaneously. The heat energy transferred to the sample was a combination of (1) the heat generated through MW coupling of the SiO_2/TiO_2 coating and (2) the heat transfer by conduction, convection and radiation from the heated susceptor to the coating and MW transparent PC substrate (Fig. 1b). Therefore, this setup provided more homogeneous heating to the sample. Compared to direct MW irradiation, where energy was partially absorbed by the coating (Fig. 1c), hybrid MW heating provided a uniform temperature distribution between the coating and the MW transparent PC substrate [14,21]. Moreover, the samples could be heated up more rapidly to the target temperature. MW irradiation could also promote hydrolysis and condensation reactions, leading to fast densification of the coating. Under MW irradiation at high temperature, unreacted Si-OH and Ti-OH underwent further condensation [14], enabling enhancement of the mechanical properties of the coating after the cladding process.

Surface morphology and coating adhesion

Morphology of the coating surfaces with different sol-gel compositions is shown in Fig. 2. Samples S1-0T, S2-5T and S3-10T show a uniform crack-free surface. However, cracks can be observed in sample S4-30T. Numerous micro-cracks can be seen on the surface of sample S6-100T. Cracking could be primarily attributed to the fast hydrolysis reaction of the TiO_2 sol during the cladding process. This produced large stresses in the coating [22], and the severity of cracking increases with increasing TiO_2 sol concentration. Therefore, the coating composition has a significant effect on the coating integrity. However, although abundant cracks were found on the surface of sample S6-100T, no detachment of the coating was observed, owing to the enhanced coating adhesion by the two-step functionization of the PC substrate. The adhesion rating and the surface morphology after the tests are shown in Table 2 and Fig. 3, respectively. The highest adhesion strength rating was recorded for the samples S1-0T, S2-5T, S3-10T and S4-30T with no coating removal. Good coating adhesion was observed as confirmed by the cross-cut test. This was due to the improved surface wettability and the surface energy of the substrate [23] by the two-step functionalization method. This process enhanced the hydrophilicity of the surface by providing active sites for chemical reaction with the coating sol during the cladding process [24,25]. Moreover, the MW cladding process may also promote the reaction between the coating sol and the surface functional group. The adhesion rating for sample S5-50T (Fig. 3b) and sample S6-100T (Fig. 3c) were specified as 4B (<5% area of removal) and 3B (5-15 % area of removal) respectively. The reduction of the adhesion rating was mainly due to the crack formation of the coating with the increase of TiO_2 content [1,16,22].

Table 2 Test result of adhesion rating.

Sample	S0	S0-2	S1-0T	S2-5T	S3-10T	S4-30T	S5-50T	S6-100T
Adhesion rating	-	-	5B	5B	5B	5B	4B	3B

The interface between the coating and substrate was investigated by SEM cross-sectional images of the samples, as shown in Fig. 4. Due to minimized temperature discrepancy between the coating and substrate, no coating delamination was observed at the interface for all the samples containing TiO_2, from S3-10T to S6-100T. Therefore, good coating adhesion could be achieved. These results showed the advantage of the hybrid MW method over the direct MW processing [17] in handling materials with different dielectric properties.

UV-VIS spectra

Optical performance and UV protection are important for a transparent substrate such as PC. To prevent photo-degradation by UV irradiation, the coating should have high optical transparency with UV absorptivity. The results of UV-visible spectra analysis in both the visible light and UV ranges for different coating compositions is shown in Fig. 5. The S1-0T coating sol shows no absorption of light within the scanning wavelength range. For all sol-gel compositions containing TiO_2, the light transmission drops drastically and reaches zero within the UV range, starting from 380 nm. The presence of TiO_2 within the coatings demonstrated good UV absorbing properties even at a low concentration of TiO_2, as in S2-5T coating sol (i.e. 5 vol.% of TiO_2). However, a further increase of TiO_2 reduces the transparency of the visible range from 380 to 700 nm, leading to an adverse effect on optical clarity to the PC substrate.

Nanomechanical performance

Sample S3-10T was used to study the nanomechanical properties of the coatings because of its crack-free surface with exceptional adherence, good optical transmittance, and UV-blocking capability compared with other compositions. Nanoindentation was conducted on the samples with 1, 3 and 5 coating layers to investigate the effect of the number of coating layers on their hardness and modulus (Fig. 6). As compared to that of the pristine PC substrate, the elastic modulus of the S3-10T samples with different number of coating layers almost doubles, increasing from 3.3 ± 0.04 GPa to 5.9 ± 0.06 GPa, while the hardness improves by over threefold, from 277.4 ± 1.5 MPa to 897.0 ± 3.5 MPa. The enhancement of the mechanical properties was mainly due to the increase in the coating thickness associcated with the increasing number of layers. This result demonstrated the remarkable improvement of mechanical performance brought by the deposition of such composite coating on the PC.

The average friction coefficients obtained during the steady nano-scratching process of the samples are summarized in Fig. 7a, with the highest friction coefficient found for the pristine PC sample, which has a value of 0.74 ± 0.03. All the three coated S3-10T samples show a significant decrease in friction coefficient compared to that of the pristine PC sample. This may be due to the rolling effect of the nanoparticles detached from the coating as proposed by Chang and Zhang [26]. The samples with 3-layer coating possess the lowest friction coefficient with a value of 0.13 ± 0.02, which implies the highest scratch resistance. This was also verified by the penetration depth in the nano-scratch test. As shown in Fig. 7b, the samples with 3-layer coating show the lowest penetration depth of 0.22 ± 0.02 μm, i.e. better resistance against scratching force. Although the coatings with 5 layers have the highest elastic modulus and hardness. During the scratching process, the stress tended to accumulate at the tip front, leading to a scratch fracture on the coating [27]. This phenomenon could be confirmed by the presence of “kinks” in the plot of the normal force against penetration depth for 5-layer coating, as compared to the plot for 3-layer coating (Fig. 8).

A comparison with a recently reported SiO_2 based protective coatings on polymer substrates is summarized in Table 3. By using the hybrid MW approach, similar mechanical properties of the coating have been achieved as compared to the findings by Le Bail *et al.* [28]. The post thermal treatment time has been significantly reduced from 1 hour to 30 s in this study. Compared with the coating fabricated through UV irradiation [29], the coating hardness was also significantly improved (about 2.5 times improvement). The results showed that the proposed protocol using hybrid microwave approach would offer a more efficient and effective method for coating fabrication.

Table 3 Comparison for recently reported hard coatings on polymer substrates.

Post-Treatment method	Post-treatment time	Hard coating materials	Nanoindentation		Ref.
			Hardness (MPa)	Elastic Modulus (GPa)	
Atmospheric plasma deposition	> 2 h	GPTMS, ZrO_2, SiO_2	670	10.6	[29]
Ventilated oven	1 h	GPTMS, ZrO_2, SiO_2	900	5.8	[22]
UV	-	urethane acrylate, SiO_2	362	5.6	[28]
MW and UV	6 min	SiO_2, TiO_2	-	-	[17]
Hybrid MW	30 s	SiO_2, TiO_2	897	5.9	This work

Conclusion

A protocol for cladding of sol-gel derived SiO_2/TiO_2 composite coatings has have been developed based on the hybrid microwave (MW) approach. It has offered homogenous heating by exploiting direct microwave and susceptor-aided heating simultaneously. The challenges of MW processing of low MW absorption composite coating on MW transparent substrate have been resolved. Good coating adhesion and surface integrity have been achieved. Scratch resistant and UV protective coatings were successfully demonstrated, and their mechanical and optical performances were verified. UV absorbability could be realized by incorporating TiO_2 into the coatings, however, increasing the content has been shown to have an adverse effect on its adhesion and scratch resistance. Coating with 10 vol. % of TiO_2 was found to be the optimal composition for the composite, resulting in a crack-free surface, as well as good clarity. With increasing numbers of coating layers, the elastic modulus and hardness drastically increased to 5.9 GPa and 897 MPa, respectively, as compared to those of the pristine PC substrate. By utilizing a two-way susceptor-aided MW heating mechanism, deposition of composite coatings with different dielectric properties have been successfully demonstrated. The hybrid MW cladding protocol would offer a fast and effective process for composite coating fabrications.

Declarations

Conflict of Interest: The authors declare that they have no conflict of interest.

References

[1] Kim N (2017) Recent progress of functional coating materials and technologies for polycarbonate. Journal of Coatings Technology and Research 14 (1):21-34

[2] Yavas H, Selçuk CDÖ, Özhan AS, Durucan C (2014) A parametric study on processing of scratch resistant hybrid sol–gel silica coatings on polycarbonate. Thin solid films 556:112-119

[3] Chantarachindawong R, Osotchan T, Chindaudom P, Srikhirin T (2016) Hard coatings for CR-39 based on Al_2O_3–ZrO_2 3-glycidoxypropyltrimethoxysilane (GPTMS) and tetraethoxysilane (TEOS) nanocomposites. Journal of Sol-Gel Science and Technology 79 (1):190-200

[4] Guglielmi M (2020) From past research experiences looking to the future of sol–gel. Journal of Sol-Gel Science and Technology:1-9

[5] Horst C, Pagno CH, Flores SH, Costa TMH (2020) Hybrid starch/silica films with improved mechanical properties. Journal of Sol-Gel Science and Technology:1-14

[6] Zhao Y, Huang C, Bei R, Su H, Wang S (2018) Barrier functionality of SiO_x layers and their effect on mechanical properties of SiO_x/PLA composite films. Journal of Coatings Technology and Research 15 (3):505-514

[7] Fajzulin I, Zhu X, Möller M (2015) Nanoparticulate inorganic UV absorbers: a review. Journal of Coatings Technology and Research 12 (4):617-632

[8] Pakdel E, Daoud WA, Sun L, Wang X (2015) Reprint of: Photostability of wool fabrics coated with pure and modified TiO_2 colloids. Journal of colloid and interface science 447:191-201

[9] Palhares HG, Gonçalves BS, Silva LMC, Nunes EHM, Houmard M (2020) Clarifying the roles of hydrothermal treatment and silica addition to synthesize TiO_2-based nanocomposites with high photocatalytic performance. Journal of Sol-Gel Science and Technology:1-17

[10] Zhang X, Zhong YL, Li L, Yan Y (2014) Adhesion failure of antiscratch coatings on polycarbonate under UV irradiation. J Appl Polym Sci 131 (15)

[11] Amirzada MR, Tatzel A, Viereck V, Hillmer H (2016) Surface roughness analysis of SiO_2 for PECVD, PVD and IBD on different substrates. Applied Nanoscience 6 (2):215-222

[12] Taeschner K, Bartzsch H, Frach P, Schultheiss E (2012) Scratch resistant optical coatings on polymers by magnetron-plasma-enhanced chemical vapor deposition. Thin Solid Films 520 (12):4150-4154

[13] Mackenzie J, Bescher E (2003) Some factors governing the coating of organic polymers by sol-gel derived hybrid materials. Journal of sol-gel science and technology 27 (1):7-14

[14] Kitchen HJ, Vallance SR, Kennedy JL, Tapia-Ruiz N, Carassiti L, Harrison A, Whittaker AG, Drysdale TD, Kingman SW, Gregory DH (2014) Modern microwave methods in solid-state inorganic materials chemistry: from fundamentals to manufacturing. Chem Rev 114 (2):1170-1206

[15] Nurdin M, Darmawati D, Maulidiyah M, Wibowo D (2018) Synthesis of Ni, N co-doped TiO_2 using microwave-assisted method for sodium lauryl sulfate degradation by photocatalyst. Journal of Coatings Technology and Research 15 (2):395-402

[16] Dinelli M, Fabbri E, Bondioli F (2011) TiO_2–SiO_2 hard coating on polycarbonate substrate by microwave assisted sol–gel technique. Journal of sol-gel science and technology 58 (2):463-469

[17] Sowntharya L, Subasri R (2013) A comparative study of different curing techniques for SiO_2–TiO_2 hybrid coatings on polycarbonate. Ceramics International 39 (4):4689-4693

[18] Mahltig B, Miao H (2017) Microwave-assisted preparation of photoactive TiO_2 on textile substrates. Journal of Coatings Technology and Research 14 (3):721-733

[19] Yoshino H, Kamiya K, Nasu H (1990) IR study on the structural evolution of sol-gel derived SiO_2 gels in the early stage of conversion to glasses. Journal of non-crystalline solids 126 (1-2):68-78

[20] Song Y, Zhuan X, Wang T, Chen X (2014) Evolution of thermal stress in a coating/substrate system during the cooling process of fabrication. Mechanics of Materials 74:26-40

[21] Bhattacharya M, Basak T (2016) A review on the susceptor assisted microwave processing of materials. Energy 97:306-338

[22] Le Bail N, Lionti K, Benayoun S, Pavan S, Thompson L, Gervais C, Dubois G, Toury B (2015) Scratch-resistant sol–gel coatings on pristine polycarbonate. New J Chem 39 (11):8302-8310

[23] Cho J-S, Han Y, Cuomo JJ (2008) Ion beam pretreatment of polymeric substrates for ITO thin film deposition. Solid state sciences 10 (7):941-949

[24] Wen J, Vasudevan V, Wilkes G (1995) Abrasion resistant inorganic/organic coating materials prepared by the sol-gel method. Journal of Sol-Gel Science and Technology 5 (2):115-126

[25] Yaghoubi H, Taghavinia N, Alamdari EK (2010) Self cleaning TiO_2 coating on polycarbonate: Surface treatment, photocatalytic and nanomechanical properties. Surface and coatings technology 204 (9-10):1562-1568

[26] Díez-Pascual AM, Diez-Vicente AL (2015) Development of linseed oil–TiO_2 green nanocomposites as antimicrobial coatings. J Mater Chem B 3 (21):4458-4471

[27] Ghermezcheshme H, Mohseni M, Yahyaei H (2015) Use of nanoindentaion and nanoscratch experiments to reveal the mechanical behavior of POSS containing polyurethane nanocomposite coatings: The role of functionality. Tribology International 88:66-75

[28] Lahijania YZK, Mohseni M, Bastani S (2014) Characterization of mechanical behavior of UV cured urethane acrylate nanocomposite films loaded with silane treated nanosilica by the aid of nanoindentation and nanoscratch experiments. Tribology International 69:10-18

[29] Ding Y, Dong S, Han J, He D, Zhao Z, Dauskardt RH (2018) Optically transparent protective coating for plastics using dual spray and atmospheric plasma deposition. Advanced Materials Interfaces 5 (9):1701433

List of figures

Fig. 1 (a) Schematic of hybrid MW cladding process, and comparison between (b) hybrid MW cladding method and (c) direct MW curing.

Fig. 2 Optical microscopy images and SEM images (inset) of (a) S1-0T, (b) S2-5T, (c) S3-10T, (d) S4-30T and (e) S6-100T samples.

Fig. 3 Optical microscopy image of (a) S3-10T, (b) S5-50T and (c) S6-100T samples after cross-cut tape test.

Fig. 4 SEM image of cross-sections (a) Sample S3-10T and (b) Sample S6-100T.

Fig. 5 UV-vis transmission spectra of different sol-gel compositions.

Fig. 6 Elastic modulus (*E*) and hardness (*H)* for pristine PC, 1 layer, 3 layers, and 5 layers of coating (S3-10T).

Fig. 7 Variation of (a) average frictional coefficient, and (b) penetration depth of pristine PC, 1 layer, 3 layers and 5 layers of coating (S3-10T) during nanoscratch test.

Fig. 8 Normal force against penetration depth for a) 3 layers and b) 5 layers of coating during nanoscratch test.

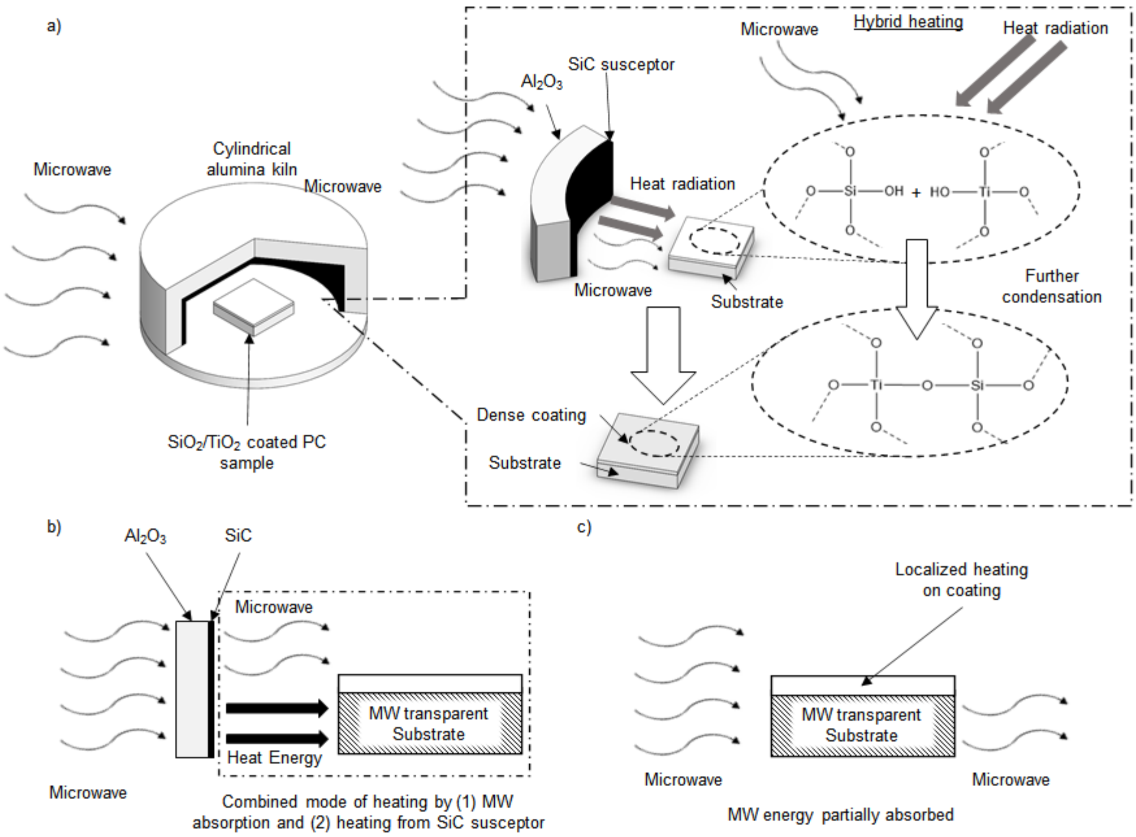

Fig. 1 (a) Schematic of hybrid MW cladding process, and comparison between (b) hybrid MW cladding method and (c) direct MW curing.

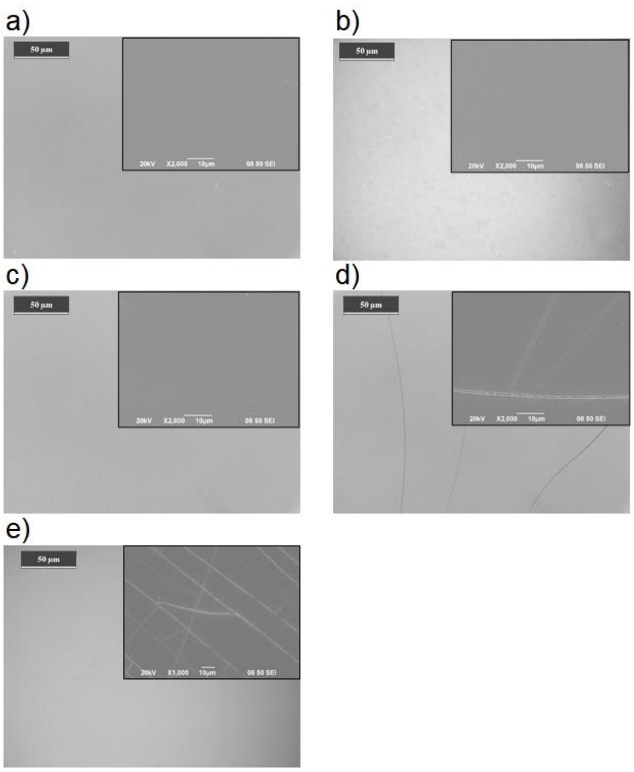

Fig. 2 Optical microscopy images and SEM images (inset) of (a) S1-0T, (b) S2-5T, (c) S3-10T, (d) S4-30T and (e) S6-100T samples.

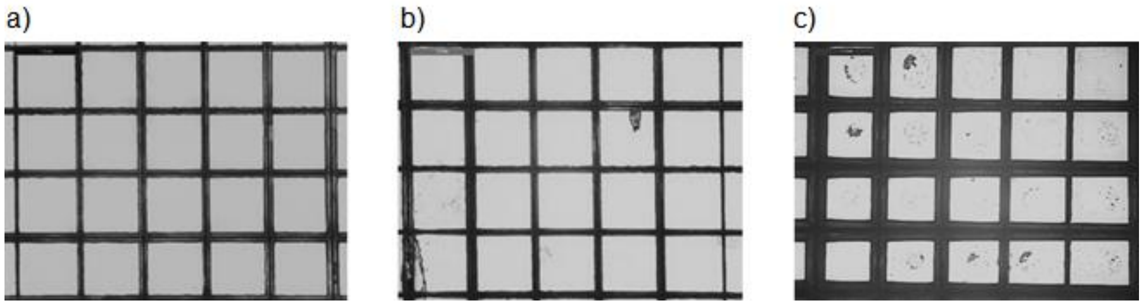

Fig. 3 Optical microscopy image of (a) S3-10T, (b) S5-50T and (c) S6-100T samples after cross-cut tape test.

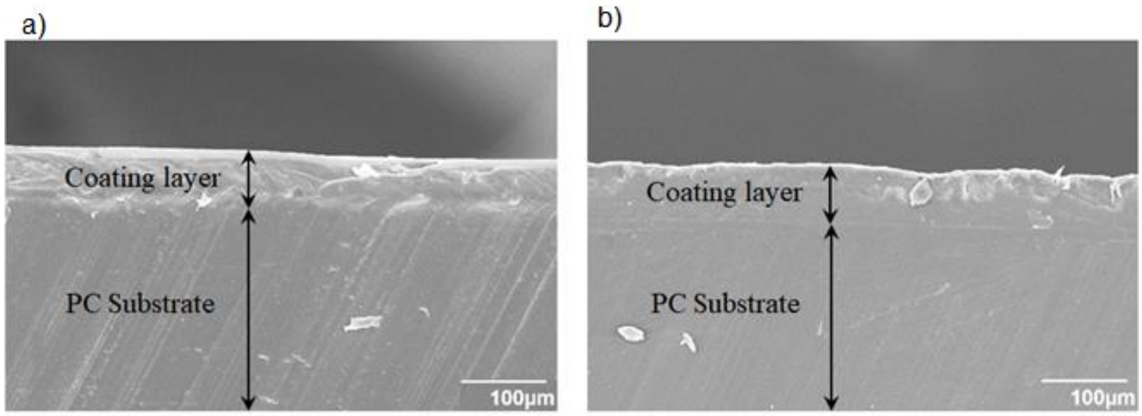

Fig. 4 SEM image of cross-sections (a) Sample S3-10T and (b) Sample S6-100T.

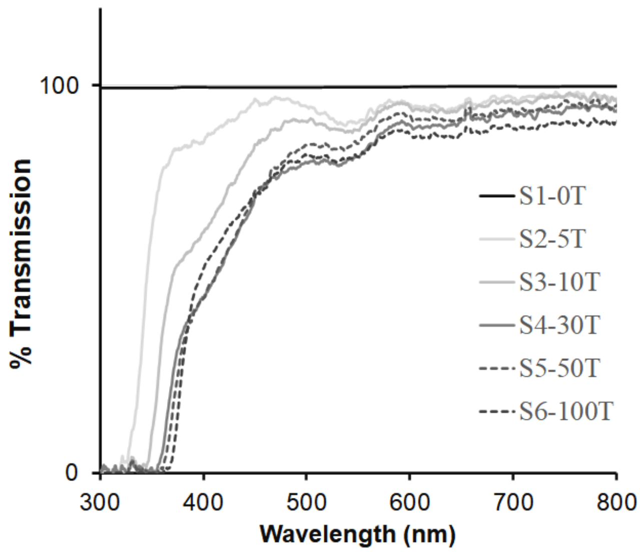

Fig. 5 UV-vis transmission spectra of different sol-gel compositions.

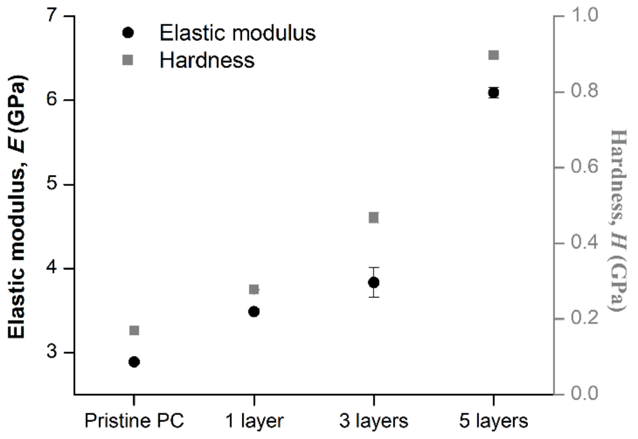

Fig. 6 Elastic modulus (*E*) and hardness (*H)* for pristine PC, and S3-10T samples with 1 layer, 3 layers, and 5 layers of the coating.

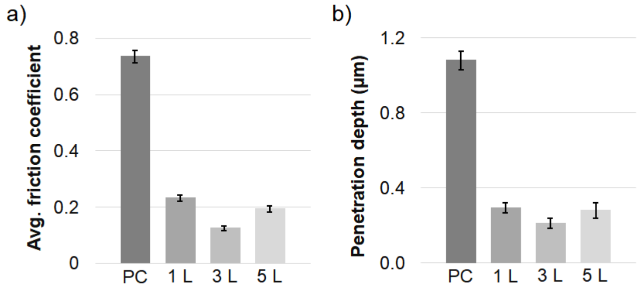

Fig. 7 Variation of (a) average frictional coefficient, and (b) penetration depth of pristine PC, and S3-10T samples with 1 layer, 3 layers and 5 layers of the coating for nano-scratch test.

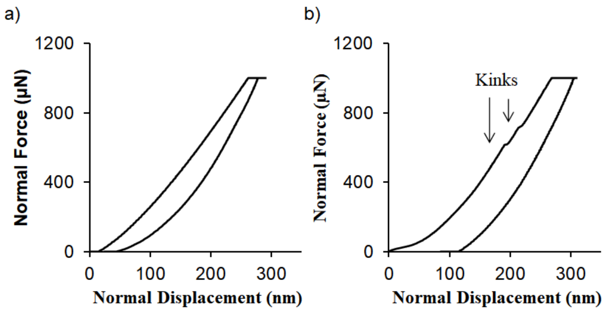

Fig. 8 Normal force against penetration depth for the S3-10T sample with a) 3 layers and b) 5 layers of the coating for nano-scratch test.